



Cite this: *React. Chem. Eng.*, 2026, 11, 64

## Mixed polyamide and polyester upcycling via chemical autoxidation and engineered *Pseudomonas putida*

Ross Eaglesfield,<sup>†ab</sup> Brandon L. Frey,<sup>†ab</sup> Ciaran W. Lahive,<sup>abc</sup> Amy A. Cuthbertson,<sup>ab</sup> Eugene Kuatsjah,<sup>‡ab</sup> Kelsey J. Ramirez,<sup>id ab</sup> Young-Saeng Avina,<sup>ab</sup> Hannah Alt,<sup>ab</sup> Natalie Banakis,<sup>d</sup> Katrina M. Knauer,<sup>id ab</sup> Gregg T. Beckham,<sup>id \*ab</sup> and Allison Z. Werner,<sup>id \*ab</sup>

Polyamides, such as nylons, are often used in multi-component materials, like textiles and packaging, and are accompanied with unique recycling challenges. Recently, autoxidation and bioconversion has emerged as a tandem approach for the conversion of mixed plastics waste to single products, however the fate of polyamides in these processes is unknown. Here, we optimized the autoxidation of nylon-6 and nylon-6,6 depolymerization, achieving >92 mol% nitrogen recovery from both substrates, predominantly as acetamide, and 20–27 mol% carbon recovery (not including acetamide). Experiments with <sup>13</sup>C-labeled acetic acid demonstrated that the carbon in acetamide was solvent derived. Autoxidation of mixed nylon-6 and poly(ethylene terephthalate) (PET) post-consumer fibers resulted in similar carbon and nitrogen recoveries from nylon, while PET was depolymerized to terephthalic acid (TPA) at >65 C-mol% recovery. Next, we engineered *Pseudomonas putida* KT2440 to utilize acetamide as the sole carbon and nitrogen source for growth through the constitutive expression of genes encoding amidase enzymes, including a native amidase (PP\_0613) shown to be active on C<sub>2</sub>–C<sub>4</sub> amides. Heterologous chromosomal expression of *amiE*, encoding the amidase from *P. aeruginosa*, was found to be superior to PP\_0613 constitutive expression in genome integrated strains. Prior engineering to enable TPA conversion to β-ketoadipate pathway intermediate protocatechuate was leveraged and combined with deletion of *pcaD* to produce muconolactone as a product. Finally, a stacked strain engineered for conversion of acetamide, TPA, and DCAs was evaluated on the reaction product from autoxidation of mixed post-consumer nylon and PET fibers without any supplemental nitrogen, achieving quantitative yields in the presence of supplemental carbon.

Received 12th August 2025,  
Accepted 9th September 2025

DOI: 10.1039/d5re00351b

rsc.li/reaction-engineering

## Introduction

Recycling of mixed plastic waste is technically challenging because of the heterogeneity in polymer chemistries, and as a result many current recycling approaches are designed for single substrates, making recycling methods that can valorize mixed feedstocks of keen interest. Catalytic autoxidation has been shown to deconstruct mixed polyesters and polyolefins<sup>1–3</sup> via C–C bond cleavage, generating soluble oxygenates,<sup>4</sup> via the

proposed generation of alkyl radicals at C–H bonds on a polymer backbone, followed by radical coupling with O<sub>2</sub> and the formation of peroxide intermediates. It is proposed these intermediates are then homolytically cleaved at the O–O bond in the presence of Co and Mn catalysts, forming alkoxy radicals that trigger β-scission of C–C bonds on the polymer backbone to generate oxygenates.<sup>4–6</sup> Of relevance to mixed feedstocks, polyamides, or nylons, are often used in blends with polyesters and other plastics especially in textiles and multi-layer packaging, and are rarely recycled. This raises the question about the fate of nylons in autoxidation.<sup>7,8</sup>

Microbial conversion of mixed oxygenates to tunable bioproducts can enable the production of higher value materials and avoid costly separations.<sup>6,9–14</sup> To this end, we previously engineered the soil bacterium *Pseudomonas putida* KT2440 (*P. putida*) to convert a mixture of oxygenates derived from autoxidation of polyethylene (PE), polystyrene (PS), and poly(ethylene terephthalate) (PET) to polyhydroxyalkanoates or β-ketoadipate (βKA).<sup>6,15,16</sup> Bioconversion of the PET monomer

<sup>a</sup> Renewable Resources and Enabling Science Center, National Renewable Energy Laboratory, Golden, CO 80401, USA. E-mail: Gregg.Beckham@nrel.gov, Allison.Werner@nrel.gov

<sup>b</sup> BOTTLE Consortium, Golden, CO 80401, USA

<sup>c</sup> Department of Materials, University of Manchester, Manchester M13 9PL, UK

<sup>d</sup> Patagonia, Inc., Ventura, CA 9300, USA

<sup>†</sup> These authors contributed equally to this work.

<sup>‡</sup> Current address: Institute Of Sustainability for Chemicals, Energy and Environment (ISCE2), Singapore 627833, Republic of Singapore.



terephthalate (TPA) has been engineered previously *via* a two-step conversion to protocatechuate,<sup>17–24</sup> a central intermediate in the  $\beta$ KA pathway.<sup>20,21,25</sup> The  $\beta$ KA pathway can be leveraged for quantitative bioconversion to a variety of performance-advantaged biochemicals,<sup>25,26</sup> such as muconolactone, which can be converted to the nylon-6 monomer, caprolactam.<sup>27</sup> Recently, *P. putida* was also engineered to catabolize the nylon-derived organonitrogen compounds 6-aminohexanoic acid,  $\epsilon$ -caprolactam, and 1,6-hexamethylenediamine.<sup>28</sup> Depending on the fate of nitrogen from nylon autoxidation, it may also be possible to utilize this liberated, waste-derived nitrogen in bioconversion applications and remove the requirement for nitrogen supplementation by other means.

In this work, we show that the oxidative depolymerization of nylon-6 yields a product mixture rich in acetamide<sup>29</sup> and short chain ( $C_4$ – $C_6$ ) dicarboxylic acids (DCAs). Mixed PET and nylon-6 yield the same nylon products, along with the generation of PET-derived TPA. We then engineered *P. putida* to utilize acetamide as a sole carbon and nitrogen source through constitutive expression of genes encoding amidase enzymes, including the native *PP\_0613* and *amiE* from *P. aeruginosa*, the

latter of which is known to be capable of deaminating acetamide to acetate and ammonium.<sup>30</sup> Building upon our previously engineered DCA-catabolizing strain,<sup>6</sup> we demonstrate complete carbon utilization and 100% molar conversion of TPA to muconolactone when grown on an effluent containing oxidative degradation products from post-consumer nylon-6 and PET waste with no supplemental nitrogen. Overall, this work provides important information on the fate of polyamides and mixed nylon-containing waste in autoxidation reactions, as well as providing a biological upcycling strategy for utilization of these breakdown products and conversion to a valuable chemical monomer.

## Results

### Chemo-catalytic oxidation of nylon-6 and nylon-6,6 yields an effluent rich in acetamide and $C_{4-6}$ DCAs

To test the effects of autoxidation on polyamides nylon-6 and nylon-6,6 (sheets sourced from Goodfellow),<sup>31</sup> we began by screening reaction conditions used in our previous work on mixed plastics deconstruction.<sup>6</sup> Specifically, acetic acid with

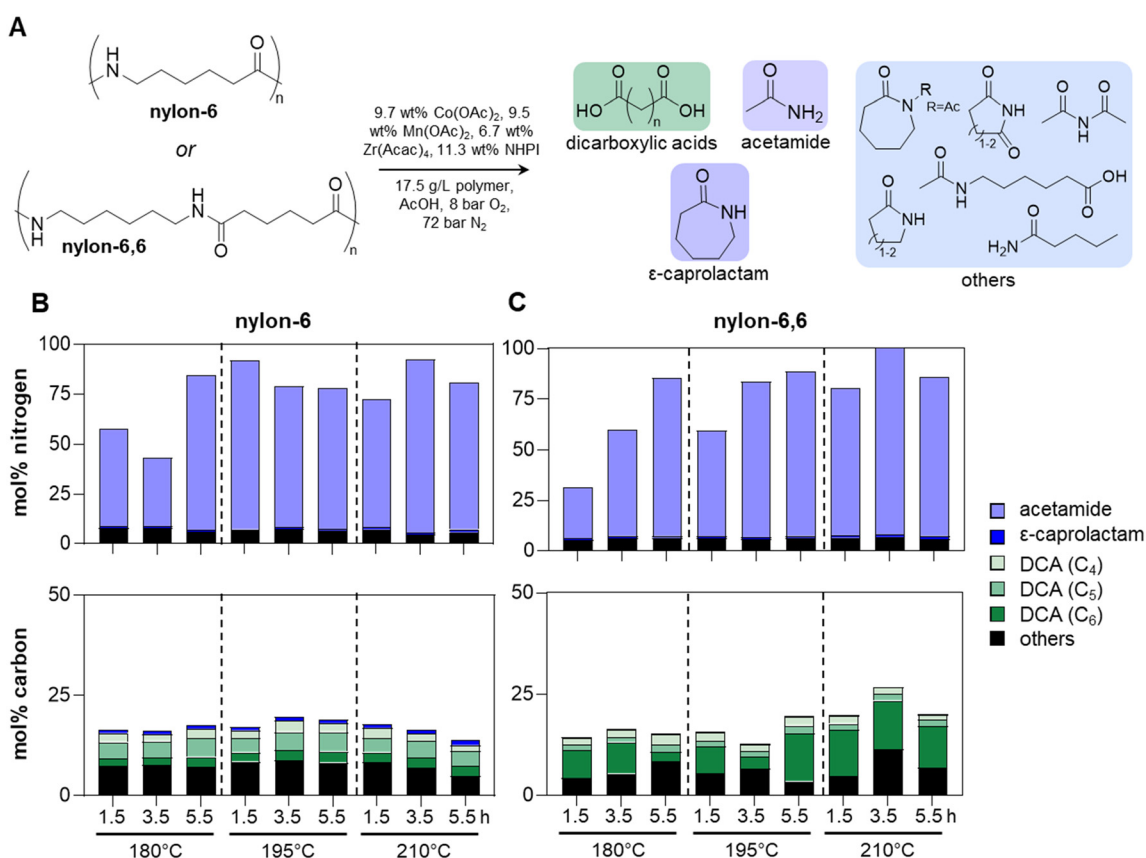


**Fig. 1** Optimization of chemo-catalytic oxidative nylon-6 and nylon-6,6 deconstruction. (A) Reaction conditions and chemical structures of starting polymers and quantified oxygenates detected following depolymerization. (B) Quantification of organonitrogen compounds and carbon-containing compounds from the autoxidation of nylon as mol% of nitrogen or carbon from the starting polymer. Acetamide is not included in carbon recovery as it is derived from the solvent. (C) Quantification of organonitrogen compounds and carbon-containing compounds from the autoxidation of nylon as mol% of either nitrogen or carbon from the starting nylon-6,6 polymer. Conditions: 350 mg of each polymer, 20 mL AcOH, Co(OAc)<sub>2</sub> (9.7 wt%), Mn(OAc)<sub>2</sub> (9.5 wt%), Zr(AcAc)<sub>4</sub> (6.7 wt%), NHPI (11.3 wt%, 24.0 mM), 8 bar O<sub>2</sub>/72 bar He. Results are from single reactions. Numerical data are provided in Excel SI 1.



Co(OAc)<sub>2</sub>, Mn(OAc)<sub>2</sub>, Zr(Acac)<sub>4</sub> as co-catalysts, and *N*-hydroxyphthalimide (NHPI) as an initiator were utilized with 38 bar air diluted with 42 bar nitrogen. Holding these reaction conditions constant, deconstruction products at reaction temperatures from 140–210 °C over 0.5–5.5 hours were quantified at 17.5 mg mL<sup>-1</sup> solids loading of nylon-6 or nylon-6,6 (Fig. 1 and S1 and S2). Molar yields were calculated as the moles of nitrogen or carbon in the quantified products (Scheme S1) relative to the nitrogen and carbon content of the starting polymers as performed in Lahive *et al.*<sup>29</sup> A complete list of identified and quantified products is provided in the SI and Excel SI 1.

Previous work investigating the oxidation products from multilayer plastic films identified acetamide as the major organonitrogen compound generated from nylon.<sup>29</sup> In our experiments acetamide accounted for up to 93.5 mol% nitrogen depending on reaction conditions.  $\epsilon$ -Caprolactam, *N*-acetylcaprolactam, 6-acetamidohexanoic acid, and diacetamide were also identified, but accounted for only a small portion of nitrogen and carbon recovery. C<sub>4</sub>–C<sub>6</sub> DCAs accounted for up to 16.0 mol% of recovered carbon (Fig. S3). Reactions above 160 °C provided high acetamide yields with the optimal conditions for the greatest nitrogen and carbon recovery, for both nylon-6 and nylon-6,6, being 210 °C for 3.5 hours (Fig. 1). Reactions at lower temperatures (140–160 °C) had lower overall nitrogen recoveries (Fig. S1 and S2), likely due to incomplete oxidation and unquantified oligomeric products. Extending the reaction time had a larger impact on yields at lower temperatures but resulted in similar nitrogen and carbon recoveries to the 210 °C, 3.5 hours optimal condition. The optimal reaction conditions yielded 92 mol% nitrogen recovery (87 mol% as acetamide) and 17 mol% carbon recovery (8 mol% as DCAs) from nylon-6, and 100 mol% total nitrogen recovery (93 mol% as acetamide) and 27 mol% carbon recovery (15 mol% as DCAs) from nylon-6,6.

To determine the origin of the carbon in acetamide, which could either be derived from the polymer or the acetic acid solvent, a reaction of nylon-6 in labeled <sup>13</sup>C<sub>2</sub>-AcOH solvent under the optimized autoxidation conditions was used. These conditions resulted solely in the production of <sup>13</sup>C<sub>2</sub>-acetamide (*m/z* = 61.04) observed *via* gas chromatograph-mass spectrometry (GC-MS), indicating that the carbon in acetamide is coming from solvent, (Fig. S4).

### Deconstruction of mixed post-consumer nylon and PET generates acetamide, DCAs, and TPA

We next examined mixed PET and nylon, including both PET powder and nylon-6 sheets from Goodfellow, and post-use fiber substrates (Fig. 2A and S5 and S6). Previously, TPA yields from PET were shown to increase at longer reaction times,<sup>6</sup> and thus we used 5.5 hours at 210 °C (Fig. 2B).

For the mixed commercial polymers, TPA yields of 79.4 ± 3.4 mol% carbon were achieved (error represents standard deviation), close to the maximum theoretical yield of 80 mol%. Nylon-derived nitrogen recovery totaled 68.7%, distributed as 61.8 ± 0.6 mol% acetamide, 3.1 ± 0.2 mol%  $\epsilon$ -caprolactam, and 3.9 ± 0.2 mol% as other organonitrogen products. Carbon recovery from nylon-6 was 44.6 ± 2.1 mol%, with 10.6 ± 1.1 mol% as DCAs, 3.1 ± 0.2 mol% as  $\epsilon$ -caprolactam and a further 30.9 ± 1.4 mol% carbon as other organonitrogen products (Fig. 2 and S5). Importantly, these data demonstrate that both acetamide and DCAs are still recovered from nylon in the presence of TPA.

The same reaction conditions were applied to mixed post-consumer polyester fibers (purple PET fleece, *M<sub>w</sub>* = 35.7 kDa, 12.9% inorganic additives) and nylon fibers (nylon-6 fishing net, *M<sub>w</sub>* = 35.1 kDa, 2.9% inorganic additives). Full substrate characterization data are in Fig. S7

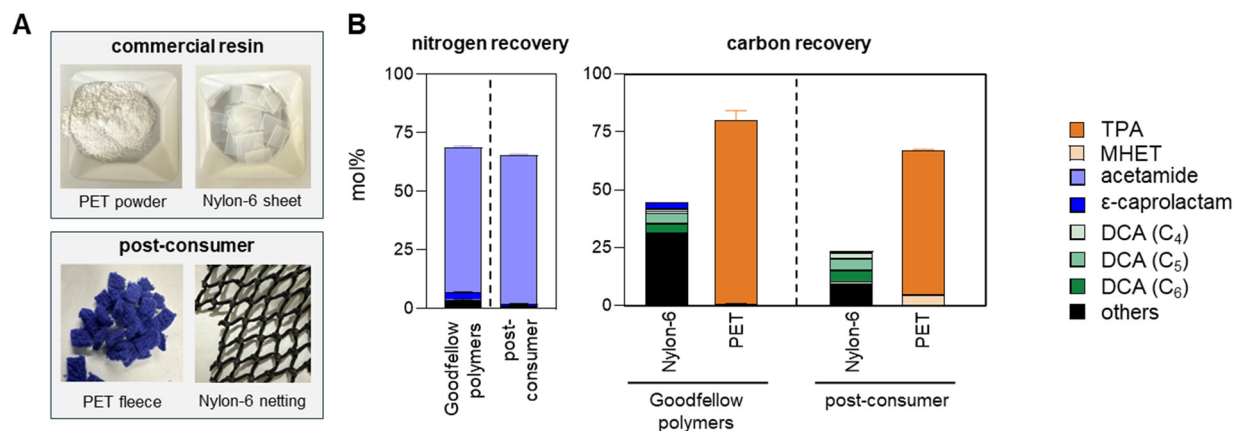


**Fig. 2** Oxidative deconstruction of mixed nylon and PET waste. (A) Polymers from Goodfellow (PET powder and nylon-6 sheet) or post-consumer materials (PET fleece and nylon-6 fishing net) were deconstructed using the following conditions: 350 mg of each polymer, 20 mL AcOH, Co(OAc)<sub>2</sub> (9.7 wt%), Mn(OAc)<sub>2</sub> (9.5 wt%), Zr(Acac)<sub>4</sub> (6.7 wt%), NHPI (11.3 wt%, 24.0 mM), 8 bar O<sub>2</sub>/72 bar He, 5.5 hours, 210 °C. (B) Nitrogen and carbon recovery as mol% from the starting polymer determined as a theoretical carbon content from the repeat unit (nitrogen recovery is all assumed to be from nylon). Stacked bars represent the mean ± SD for each chemical species from 4–5 independent reactions. Numerical data are provided in Excel SI 1.



and S8. Both the product distribution and yields were similar to commercial polymers, with a nitrogen and carbon recovery of  $65.4 \pm 0.4$  mol% and  $24.2 \pm 2.5$  mol%, respectively from nylon-6, and a TPA yield of  $62.8 \pm 0.4$  mol% from PET (Fig. 2 and S6).

### PP\_0613 is an amidase in *P. putida*, the constitutive expression of which enables growth on acetamide

We next sought to develop *P. putida* for biological funneling<sup>32,33</sup> of the PET- and nylon-derived oxygenates. Having previously engineered DCA and TPA catabolism in *P. putida*,<sup>6,20</sup> we first evaluated whether *P. putida* natively catabolizes acetamide. Wild-type *P. putida* did not display growth or utilization of acetamide when provided in M9 minimal medium as a sole carbon source or in addition to glucose (Fig. 3B and S9–S13). Notably, *P. putida* proteins PP\_0613, PP\_2932, and PP\_5629 are annotated as amidase family proteins, presenting the potential to convert acetamide to ammonium and acetate. Acetate could then be converted to acetyl-CoA *via* AcsA<sup>34</sup> to support growth while ammonium could be used as a nitrogen source directly (Fig. 3E).

To evaluate this, we constitutively expressed *PP\_0613*, *PP\_2932*, or *PP\_5629* from the pBTL-2 replicative plasmid<sup>35</sup> in *P. putida*, generating strains YC039, YC042, and YC045, respectively (Tables 1 and S1–S4). During cultivation in M9 minimal media supplemented with 50 mM acetamide as the sole carbon source, YC039 grew, albeit slowly (Fig. S9), suggesting *PP\_0613*, but not *PP\_2932* or *PP\_5629*, conducts acetamide deamination. Increasing acetamide concentrations in the media reduced the lag time and increased the growth rate up to the maximal tested concentration of 200 mM (Fig. 3A and S10). Acetamide quantitation confirmed that YC039 growth on acetamide as the sole carbon source occurred simultaneously with acetamide depletion (Fig. 3C). Additionally, co-feeding with glucose had little effect on acetamide utilization in YC039 (Fig. S11).

To further confirm *PP\_0613* as an amidase, we performed an *in vitro* assay using purified protein. *PP\_0613* or bovine serum albumin (BSA) as a negative control was incubated with the C<sub>2–4</sub> amides acetamide, propylamide, or butanamide and formation of the corresponding acid was determined by high performance liquid chromatography (HPLC). *PP\_0613* converted all the tested amides into their corresponding acids, confirming its activity as a short-chain amidase (Fig. 3F).

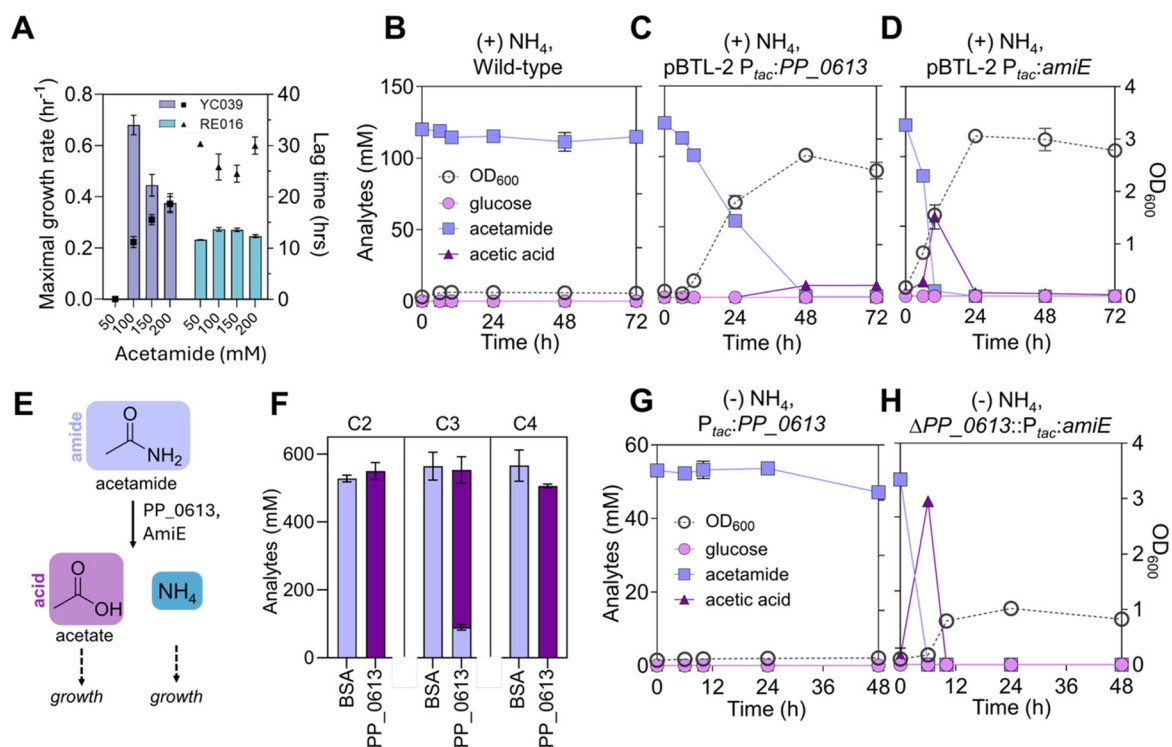


**Fig. 3** Constitutive expression of amidase enzymes for acetamide utilization in *P. putida*. (A) Lag phase (bars) and maximum growth rate (symbols) of strains YC039 and RE016 grown in microtiter plates with acetamide as the sole carbon source and  $1 \text{ g L}^{-1}$   $\text{NH}_4\text{Cl}$  added as supplemental nitrogen. (B–D) Growth ( $\text{OD}_{600}$ ) and metabolite quantification of (B) wild-type *P. putida*, (C) YC039, and (D) RE016 grown in shake flasks containing 130 mM acetamide as the sole carbon source and  $1 \text{ g L}^{-1}$   $\text{NH}_4\text{Cl}$  added as supplemental nitrogen. (E) Schematic of proposed amidase-mediated deamination of acetamide to acetate and ammonium. (F) Purified *PP\_0613* *in vitro* amidase assay. Protein was incubated with C<sub>2</sub>–C<sub>4</sub> amides and production of the corresponding acid was measured by HPLC. Bovine serum albumin (BSA) is used as a negative control. (G and H) Growth ( $\text{OD}_{600}$ ) and metabolite quantification of (G) RE026 and (H) RE020 grown in shake flasks containing 50 mM acetamide as the sole carbon and nitrogen source. All data are the mean  $\pm$  SD from three independent biological replicates. Genotypes are provided in Table 1 and numerical data are provided in Excel S1.



**Table 1** Selected strains utilized in this study. A full list with corresponding construction details are provided in Tables S1–S4

Strain	Genotype	Ref.
<i>P. putida</i> AW162	Wild-type <i>Pseudomonas putida</i> KT2440 <i>P. putida</i> KT2440 $\Delta$ hsdM-hsdR::P <sub>tac</sub> :tphA2 <sub>II</sub> :A3 <sub>II</sub> :B <sub>II</sub> :A1 <sub>II</sub> f <sub>pVA</sub> :P <sub>tac</sub> :tpaK $\Delta$ gclR P <sub>tac</sub> :glcDEFG:PP_3749 $\Delta$ paaX::P <sub>tac</sub> :dcaAKIJP(CO) $\Delta$ psrA	ATCC® 47054 6
YC039	<i>P. putida</i> KT2440 + pAW074 (pBTL2-based expression of PP_0613)	This work
YC042	<i>P. putida</i> KT2440 + pAW075 (pBTL2-based expression of PP_2932)	This work
YC045	<i>P. putida</i> KT2440 + pAW076 (pBTL2-based expression of PP_5629)	This work
RE016	<i>P. putida</i> KT2440 + pRE003 (pBTL2-based expression of <i>amiE</i> )	This work
RE020	<i>P. putida</i> KT2440 $\Delta$ PP_0613::P <sub>tac</sub> : <i>amiE</i>	This work
RE026	<i>P. putida</i> KT2440 P <sub>tac</sub> :PP_0613	This work
RE093	<i>P. putida</i> KT2440 $\Delta$ hsdM-hsdR::P <sub>tac</sub> :tphA2 <sub>II</sub> :A3 <sub>II</sub> :B <sub>II</sub> :A1 <sub>II</sub> f <sub>pVA</sub> :P <sub>tac</sub> :tpaK $\Delta$ gclR P <sub>tac</sub> :glcDEFG:PP_3749 $\Delta$ paaX::P <sub>tac</sub> :dcaAKIJP(CO) $\Delta$ psrA $\Delta$ PP_0613::P <sub>tac</sub> : <i>amiE</i> $\Delta$ pcaD	This work

### Constitutive expression of amidase *amiE* from *P. aeruginosa* results in faster acetamide utilization compared to PP\_0613

Given the modest growth rate of cells constitutively expressing PP\_0613, especially at low acetamide concentrations (Fig. 3A), we investigated heterologous expression of the AmiE amidase from *P. aeruginosa*, which can deaminate acetamide in this bacterium.<sup>36</sup> Constitutive expression of *amiE* on pBTL-2 (strain RE016) resulted in reduced lag and superior growth on all acetamide concentrations compared to YC039 (Fig. 3A), and faster acetamide utilization as the sole carbon source (Fig. 3D). Acetate was again detected following acetamide utilization and, like YC039, the addition of acetamide alongside glucose led to increased levels of growth (Fig. S11 and S12). Acetamide utilization appeared relatively unaffected by the presence of glucose (Fig. S11).

### Chromosomal constitutive expression of *amiE* enables growth on acetamide as the sole carbon and nitrogen source

To remove the requirement for antibiotic addition, we next tested the chromosomal constitutive expression of PP\_0613 and *amiE*. The strong constitutive *tac* promoter (P<sub>tac</sub>) was integrated in front of PP\_0613, which is the second gene in a two-gene operon with PP\_0614. A terminator sequence was inserted between the PP\_0614 coding sequence and the heterologous P<sub>tac</sub> to insulate expression of PP\_0613, thus generating strain RE026. A second strain, RE020, was generated by replacing the coding sequence of PP\_0613 with the *amiE* gene again under the control of an insulated P<sub>tac</sub>.

Microtiter growth experiments showed that RE026 was unable to grow on acetamide at any of the tested concentrations whereas RE020 grew on 50–150 mM acetamide as the sole carbon source (Fig. S12 and S13). In shake flask experiments containing no exogenous nitrogen source other than acetamide, RE026 was again unable to grow on acetamide, but showed some acetamide utilization after >24 hours when fed with glucose (Fig. 3G and S14). Conversely, RE020 fully metabolized acetamide within 6 hours, and consumption was again followed by production and subsequent utilization of acetate (within 10 hours) from the breakdown of acetamide (Fig. 3H). Supplementation with glucose did not impact acetamide

utilization and allowed higher maximum OD<sub>600</sub> levels (Fig. S13 and S14). Taken together, these data suggest that chromosomal integration of *amiE* but not PP\_0613 facilitates efficient conversion of acetamide and growth of engineered *P. putida* in minimal media containing no additional nitrogen or carbon.

### Engineered *P. putida* produces muconolactone at theoretical yields from oxidatively deconstructed post-consumer mixed PET and nylon-6 waste without supplemental nitrogen

With the ability to utilize acetamide as the sole carbon and nitrogen source, we next generated a strain capable of concomitantly utilizing acetamide and DCAs from nylon as well as converting TPA from the breakdown of PET into muconolactone. To this end, we took a strain previously engineered in our group for the efficient catabolism of DCAs and TPA (strain AW162), chromosomally overexpressed *amiE*, and knocked out *pcaD*, which encodes the 3-oxoadipate enol-lactonase that converts muconolactone to  $\beta$ -ketoadipate, resulting in strain RE093 (Fig. 4A).

To prepare the polymer-derived oxygenates for bioconversion, the effluent from post-consumer mixed PET and nylon-6 chemo-catalytic autoxidation was dried to remove residual acetic acid, pH adjusted to ~11.5 with 4 N NaOH to precipitate metals and solubilize small molecules, 0.2  $\mu$ m-filtered to sterilize and recover the catalyst, and re-analyzed for substrate distribution (Fig. 4B). This substrate was supplied to bacterial cultivations at two concentrations corresponding to 35.8 and 17.9 mM of quantified reaction-derived organic carbon, either alone or with glucose supplementation to provide additional cellular energy and carbon to support bioconversion. In all cases, acetamide provided the only source of nitrogen for cellular growth.

Muconolactone production at 85.9  $\pm$  2.9 mol% yield was observed at the higher effluent concentration when glucose was supplemented (Fig. 4C). Poor growth and bioconversion were observed without glucose supplementation at the higher effluent concentration (Fig. 4C and S15), suggesting an additional carbon and/or energy source is needed to mitigate toxicity at 35.8 mM quantified organic carbon. We subsequently



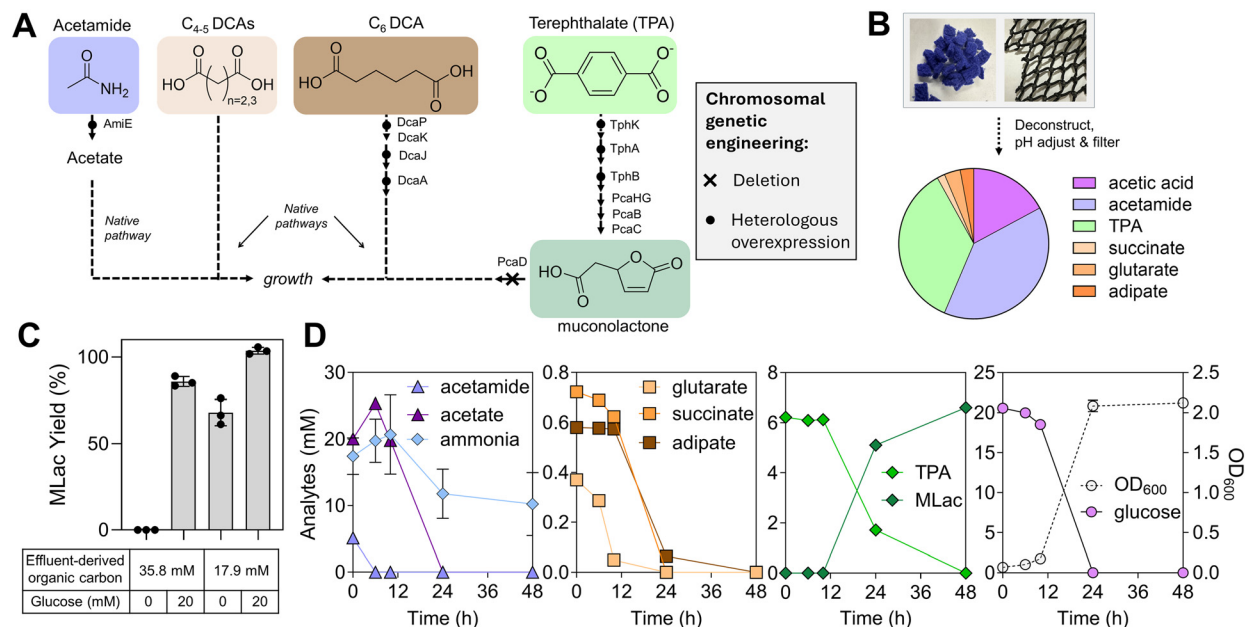


**Fig. 4** Biological funneling of autoxidation products from mixed PET and nylon depolymerization to muconolactone. (A) Engineered metabolic pathways in *P. putida* for utilization of nylon-derived oxygenates for growth and conversion of TPA to muconolactone. (B) Substrates present in the autoxidation effluent following the removal of residual catalysts and pH balancing. (C) Molar yield of muconolactone from TPA in various effluent concentrations and highlighting the effects of glucose supplementation on yield. (D) Substrate utilization, growth (OD<sub>600</sub>), and muconolactone production by strain RE093 grown in effluent plus 20 mM glucose. All data are the mean  $\pm$  SD from three independent biological replicates. Genotypes are provided in Table 1 and numerical data are provided in Excel S1.

ruled out the high levels of residual acetic acid in samples as the cause (Fig. S16).

At the lower effluent concentration, muconolactone was produced at  $68.0 \pm 7.6$  and  $103.7 \pm 1.9$  mol% yields in the absence and presence of supplemental glucose, respectively. In the glucose-supplemented case, acetamide and acetic acid were both fully utilized by 6 and 24 h respectively, while a spike in ammonia was detected and subsequently consumed during cellular growth (Fig. 4D). DCAs and glucose were consumed by  $\sim 24$  h with cells reaching stationary phase after consumption, and TPA was fully converted to muconolactone by 48 h. Together these data show that our engineered strain RE093 utilized mixed oxygenates from the oxidative depolymerization of post-consumer nylon-6 and PET mixtures, maintained growth without nitrogen supplementation *via* the deamination of acetamide, and produced muconolactone from TPA at quantitative molar yields.

## Discussion and conclusions

Recycling of synthetic fibers and multi-layer packaging is challenging in part due to the presence of mixed polymers, *e.g.*, polyester and polyamide, as well as the incompatibility of many of these polymers with current recycling technologies. Here, we demonstrate chemo-catalytic autoxidation of mixed PET and nylon-6 followed by biological valorization to muconolactone. Our method leverages previous work in oxidative depolymerization of mixed plastic waste streams<sup>6</sup> paired with an engineered strain of *P. putida*, now capable of utilizing

acetamide, the major nitrogen-containing deconstruction product from nylon, as a carbon and nitrogen source. The final strain converted TPA from post-consumer deconstruction effluents to muconolactone at quantitative yields. Muconolactone is a platform molecule for nylon monomers such as adipic acid and caprolactam,<sup>27</sup> thus providing a proof-of-concept for nylon-containing mixed polymer upcycling.

With respect to chemo-catalytic reactions, our results indicate that DCAs are recoverable (albeit at modest yields) from nylons, even at the forcing reaction conditions required for PET depolymerization (Fig. 1 and S1–S3). At the laboratory scale these reactions are performed with non-recovered catalysts, it would however be interesting in the future to consider catalyst recovery and re-use, given the interest in this chemistry for plastics deconstruction more generally.<sup>37</sup> Notably in the present work, the autoxidation of nylon-6 in labelled <sup>13</sup>C<sub>2</sub>-acetic acid confirmed that the carbon in acetamide was generated by the acetic acid solvent (Fig. S4), although the mechanism for this transformation was not determined. As shown in Scheme S2 in the SI, we hypothesize that acetamide is produced *via* acid-catalyzed acidolysis of an acetamide group on the polymer chain to generate a *N*-acyl functional group, followed by C–H abstraction of the alpha hydrogen, peroxide formation, and  $\beta$ -scission at the C–N bond to generate the free acetamide. This deleterious consumption of solvent renders the prospect of autoxidation of pure nylon unsuitable, however, in polymer blends containing low quantities of nylon, as is often the case for textiles and multilayer packaging, minor solvent consumption would likely not be substantial, and the benefits



of recovering a bio-available nitrogen source for a subsequent bioprocess should not be overlooked.

We discovered that the *P. putida* *PP\_0613* gene encodes an amidase capable of deamination of C<sub>2</sub>–C<sub>4</sub> amides, supported by *in vitro* assays and plasmid-based constitutive expression in *P. putida* (Fig. 3). However, unlike for plasmid-based expression, a strain chromosomally overexpressing *PP\_0613* did not grow on acetamide as the sole carbon and nitrogen source and utilized only a small amount of acetamide in the presence of glucose. Whole-genome sequencing showed no mutations in either the promoter region or the ribosome binding site and *in silico* analysis predicted similar transcription initiation rates, so we speculate that the reduced copy number going from plasmid to genome-integrated strains underpins this observation.<sup>35</sup> It may also be possible that the native substrate of *PP\_0613* is not acetamide, requiring further biochemical analysis.

In cultivations on effluent from post-consumer PET and nylon-6, we observed a concentration-dependent increase in lag, decrease in substrate utilization, and reduction in muconolactone yields (Fig. 4 and S15), suggesting an unknown component is presenting cellular stress.<sup>39</sup> This is unlikely due to acetate, present as residual solvent and known to have inhibitory effects due to ionic imbalance within the cell,<sup>40,41</sup> as the growth and TPA utilization in RE093 cultivations was unaffected by up to 40 mM acetate (Fig. S16). The PET fleece and nylon fishing net contained 12.9% and 2.9% inorganic additives, respectively, and both contained colorants (likely an azo-based dye in the PET fleece, and carbon black in the fishing net), presenting the possibility that these additives may present toxicity. Glucose supplementation mitigated these issues here but is an expensive process input. Notably, the addition of other plastic feedstocks could increase cellular carbon and energy, or muconolactone precursors (*e.g.*, benzoate from PS<sup>6</sup>) but also present other additives. Future work engineering improved microbial tolerance to and/or utilization of these additives, as well as further understanding the source of toxicity effects, would improve bioprocess robustness.

For the scope of this work, we focused on engineering the utilization of acetamide given the abundance of this molecule in our deconstructed nylon effluent. Other molecules are however present, such as  $\epsilon$ -caprolactam and other amide-containing molecules (Fig. 1, Scheme S1), albeit at low levels. Recent work has shown that *P. putida* can be engineered, enabled by adaptive laboratory evolution, to utilize  $\epsilon$ -caprolactam and other amide-containing molecules 1,6-hexamethylenediamine and 6-aminohexanoic acid.<sup>28</sup> Another study has shown the degradation of toxic amides such as acrylamide by *P. putida* through the constitutive expression of a unique amidase from *P. stutzeri*.<sup>42</sup> While not directly related to the amides present in our work, the apparent promiscuity of this enzyme makes it an interesting candidate for further study. Future work could leverage these recent advances to further increase the carbon closure from biological funneling of mixed substrate autoxidation effluents. In addition, further strain engineering should be performed to enhance acetate and TPA utilization.<sup>17,18,24,38</sup>

## Materials and methods

Detailed materials and methods can be found in the ESI.

## Author contributions

RE, conceptualization, data curation, data analysis and visualization, design of experiments, writing – original draft, review & editing. BLF, conceptualization, data analysis and visualization, design of experiments, writing – original draft, review & editing. CWL, conceptualization, performance of experiments, data analysis. EK, data curation. KJR, data analysis. YSA, data curation, data analysis, design of experiments. HA, data analysis. AAC, data curation and analysis. GTB conceptualization, project administration, supervision, funding acquisition, writing, review & editing. AZW conceptualization, project administration, design of experiments, supervision, funding acquisition, writing, review & editing.

## Conflicts of interest

R. E., B. L. F., C. W. L., G. T. B., and A. Z. W. have filed a patent application on the engineered strains and chemocatalytic reaction conditions reported in this work.

## Data availability

Supplementary information: The data supporting this article are available in Excel File S1 and the SI, along with additional materials, figures, and tables. See DOI: <https://doi.org/10.1039/D5RE00351B>.

The data supporting this article have been included as part of the SI.

## Acknowledgements

This work was supported by the U.S. Department of Energy, Office of Energy Efficiency and Renewable Energy, Advanced Materials and Manufacturing Technologies Office (AMMTO) and Bioenergy Technologies Office (BETO). This work was performed as part of the Bio-Optimized Technologies to keep Thermoplastics out of Landfills and the Environment (BOTTLE) Consortium and was supported by AMMTO and BETO under Contract DE-AC36-08GO28308 with the National Renewable Energy Laboratory (NREL), operated by Alliance for Sustainable Energy, LLC. We would like to thank Clarissa Lincoln for her work on GPC, Lisa M. Stanley for her work on TGA, Kevin P. Sullivan for his knowledge of textiles, and Gloria Rossetto for her work on muconolactone.

## References

- 1 A. Pifer and A. Sen, *Angew. Chem., Int. Ed.*, 1998, **37**, 3306–3308.
- 2 L. D. Ellis, N. A. Rorrer, K. P. Sullivan, M. Otto, J. E. McGeehan, Y. Román-Leshkov, N. Wierckx and G. T. Beckham, *Nat. Catal.*, 2021, **4**, 539–556.



- 3 S. Oh and E. E. Stache, *Chem. Soc. Rev.*, 2024, **53**, 7309–7327.
- 4 W. Partenheimer, *Catal. Today*, 2003, **81**, 117–135.
- 5 I. Hermans, P. A. Jacobs and J. Peeters, *J. Mol. Catal. A: Chem.*, 2006, **251**, 221–228.
- 6 K. P. Sullivan, A. Z. Werner, K. J. Ramirez, L. D. Ellis, J. R. Bussard, B. A. Black, D. G. Brandner, F. Bratti, B. L. Buss, X. Dong, S. J. Haugen, M. A. Ingraham, M. O. Konev, W. E. Michener, J. Miscall, I. Pardo, S. P. Woodworth, A. M. Guss, Y. Román-Leshkov, S. S. Stahl and G. T. Beckham, *Science*, 2022, **378**, 207–211.
- 7 N. Yanagihara and K. Ohgane, *Polym. Degrad. Stab.*, 2013, **98**, 2735–2741.
- 8 V. Hirschberg and D. Rodrigue, *J. Polym. Sci.*, 2023, **61**, 1937–1958.
- 9 J. G. Linger, D. R. Vardon, M. T. Guarnieri, E. M. Karp, G. B. Hunsinger, M. A. Franden, C. W. Johnson, G. Chupka, T. J. Strathmann, P. T. Pienkos and G. T. Beckham, *Proc. Natl. Acad. Sci. U. S. A.*, 2014, **111**, 12013–12018.
- 10 M. W. Guzik, S. T. Kenny, G. F. Duane, E. Casey, T. Woods, R. P. Babu, J. Nikodinovic-Runic, M. Murray and K. E. O'Connor, *Appl. Microbiol. Biotechnol.*, 2014, **98**, 4223–4232.
- 11 S. Lee, Y. R. Lee, S. J. Kim, J.-S. Lee and K. Min, *Chem. Eng. J.*, 2023, **454**, 140470.
- 12 C. Rabot, Y. Chen, S. Y. Lin, B. Miller, Y. M. Chiang, C. E. Oakley, B. R. Oakley, C. C. C. Wang and T. J. Williams, *J. Am. Chem. Soc.*, 2023, **145**, 5222–5230.
- 13 C. Rabot, Y. Chen, S. Bijlani, Y.-M. Chiang, C. E. Oakley, B. R. Oakley, T. J. Williams and C. C. C. Wang, *Angew. Chem., Int. Ed.*, 2023, **62**, e202214609.
- 14 R. R. Klauer, D. A. Hansen, D. Wu, L. M. O. Monteiro, K. V. Solomon and M. A. Blenner, *Annu. Rev. Chem. Biomol. Eng.*, 2024, **15**, 315–342.
- 15 N. A. Rorrer, S. F. Notonier, B. C. Knott, B. A. Black, A. Singh, S. R. Nicholson, C. P. Kinchin, G. P. Schmidt, A. C. Carpenter, K. J. Ramirez, C. W. Johnson, D. Salvachúa, M. F. Crowley and G. T. Beckham, *Cell Rep. Phys. Sci.*, 2022, **3**, 100840.
- 16 R. M. Cywar, N. A. Rorrer, C. B. Hoyt, G. T. Beckham and E. Y. X. Chen, *Nat. Rev. Mater.*, 2022, **7**, 83–103.
- 17 M. Sasoh, E. Masai, S. Ishibashi, H. Hara, N. Kamimura, K. Miyauchi and M. Fukuda, *Appl. Environ. Microbiol.*, 2006, **72**, 1825–1832.
- 18 H. Hara, L. D. Eltis, J. E. Davies and W. W. Mohn, *J. Bacteriol.*, 2007, **189**, 1641–1647.
- 19 S. Yoshida, K. Hiraga, T. Takehana, I. Taniguchi, H. Yamaji, Y. Maeda, K. Toyohara, K. Miyamoto, Y. Kimura and K. Oda, *Science*, 2016, **351**, 1196–1199.
- 20 A. Z. Werner, R. Clare, T. D. Mand, I. Pardo, K. J. Ramirez, S. J. Haugen, F. Bratti, G. N. Dexter, J. R. Elmore, J. D. Huenemann, G. L. t. Peabody, C. W. Johnson, N. A. Rorrer, D. Salvachua, A. M. Guss and G. T. Beckham, *Metab. Eng.*, 2021, **67**, 250–261.
- 21 T. Tiso, T. Narancic, R. Wei, E. Pollet, N. Beagan, K. Schroder, A. Honak, M. Jiang, S. T. Kenny, N. Wierckx, R. Perrin, L. Averous, W. Zimmermann, K. O'Connor and L. M. Blank, *Metab. Eng.*, 2021, **66**, 167–178.
- 22 T. Narancic, M. Salvador, G. M. Hughes, N. Beagan, U. Abdulmutalib, S. T. Kenny, H. Wu, M. Saccomanno, J. Um, K. E. O'Connor and J. I. Jimenez, *Microb. Biotechnol.*, 2021, **14**, 2463–2480.
- 23 S. M. You, S. S. Lee, M. H. Ryu, H. M. Song, M. S. Kang, Y. J. Jung, E. C. Song, B. H. Sung, S. J. Park, J. C. Joo, H. T. Kim and H. G. Cha, *RSC Adv.*, 2023, **13**, 14102–14109.
- 24 A. Z. Werner, Y.-S. C. Avina, J. Johnsen, F. Bratti, H. M. Alt, E. T. Mohamed, R. Clare, T. D. Mand, A. M. Guss, A. M. Feist and G. T. Beckham, *Metab. Eng.*, 2025, **88**, 196–205.
- 25 C. S. Harwood and R. E. Parales, *Annu. Rev. Microbiol.*, 1996, **50**, 553–590.
- 26 C. W. Johnson, D. Salvachúa, N. A. Rorrer, B. A. Black, D. R. Vardon, P. C. St. John, N. S. Cleveland, G. Dominick, J. R. Elmore, N. Grundl, P. Khanna, C. R. Martinez, W. E. Michener, D. J. Peterson, K. J. Ramirez, P. Singh, T. A. VanderWall, A. N. Wilson, X. Yi, M. J. Bidy, Y. J. Bomble, A. M. Guss and G. T. Beckham, *Joule*, 2019, **3**, 1523–1537.
- 27 L. Coudray, V. Bui, J. W. Frost and D. Schweitzer, *US Pat.*, US2013/00852.55A1, 2013.
- 28 J. de Witt, T. Luthe, J. Wiechert, K. Jensen, T. Polen, A. Wirtz, S. Thies, J. Frunzke, B. Wynands and N. Wierckx, *Nat. Microbiol.*, 2025, **10**, 667–680.
- 29 C. W. Lahive, A. A. Cuthbertson, A. N. Walsh, S. E. Reiber, H. M. Alt, B. A. Black, C. Botello, J. S. DesVeaux, S. Lask, C. Lincoln, W. E. Michener, J. Miscall, K. J. Ramirez, L. M. Stanley, S. P. Woodworth, S. S. Stahl and T. Beckham Gregg, Catalytic autoxidation for depolymerization of multilayer films, In Preparation, 2025.
- 30 R. Pacheco, A. Karmali, M. L. Serralheiro and P. I. Haris, *Anal. Biochem.*, 2005, **346**, 49–58.
- 31 A. A. Cuthbertson, C. Lincoln, J. Miscall, L. M. Stanley, A. K. Maurya, A. S. Asundi, C. J. Tassone, N. A. Rorrer and G. T. Beckham, *Green Chem.*, 2024, **26**, 7067–7090.
- 32 Y. Chainani, G. Bonanzio, K. E. Tyo and L. J. Broadbelt, *Curr. Opin. Biotechnol.*, 2023, **84**, 102992.
- 33 A. Z. Werner and L. D. Eltis, *Trends Biotechnol.*, 2023, **41**, 270–272.
- 34 S. Yang, S. Li and X. Jia, *J. Ind. Microbiol. Biotechnol.*, 2019, **46**, 793–800.
- 35 M. D. Lynch and R. T. Gill, *Biotechnol. Bioeng.*, 2006, **94**, 151–158.
- 36 S. A. Wilson and R. E. Drew, *J. Bacteriol.*, 1995, **177**, 3052–3057.
- 37 R. A. F. Tomás, J. C. M. Bordado and J. F. P. Gomes, *Chem. Rev.*, 2013, **113**, 7421–7469.
- 38 K. Y. Choi, D. Kim, W. J. Sul, J. C. Chae, G. J. Zylstra, Y. M. Kim and E. Kim, *FEMS Microbiol. Lett.*, 2005, **252**, 207–213.
- 39 P. G. Hamill, A. Stevenson, P. E. McMullan, J. P. Williams, A. D. R. Lewis, S. S. K. E. Stevenson, K. D. Farnsworth, G. Khroustalyova, J. Y. Takemoto, J. P. Quinn, A. Rapoport and J. E. Hallsworth, *Sci. Rep.*, 2020, **10**, 5948.
- 40 S. Pinhal, D. Ropers, J. Geiselmann and H. de Jong, *J. Bacteriol.*, 2019, **201**(13), DOI: [10.1128/jb.00147-19](https://doi.org/10.1128/jb.00147-19).
- 41 S. Mutyala and J. R. Kim, *Bioresour. Technol.*, 2022, **364**, 128064.
- 42 H. Jiang, X. Yu, J. Guo, G. Shang and Y. Dai, *J. Agric. Food Chem.*, 2024, **72**, 2109–2119.

